JOURNAL OF MATERIALS SCIENCE 19 (1984) 1629–1637

Dislocations in energetic materials

Part 3 *Etching and microhardness studies of pentaerythritol tetranitrate and cyclotrimethylenetrinitramine*

P. J. HALFPENNY*, K. J. ROBERTS, J. N. SHERWOOD
Department of Pure and Applied Chemistry, University of Strathclyde, Glasgow, UK

An assessment has been made of the primary dislocation slip systems in the explosives pentaerythritol tetranitrate (PETN) and cyclotrimethylene trinitramine (RDX) using a combination of dislocation etching and microhardness indentation techniques. Hardness measurements were made on all major habit faces as a function of temperature and load. These showed that, within the attainable temperature range (PETN 293 to 353 K, RDX 293 to 373 K) no change in hardness occurred which could be associated with the development of deformation mechanisms additional to those operating at room temperature. The hardness values of both materials were consistent with values obtained in some previous measurements (PETN 17 kg mm^{-2}, RDX 39 kg mm^{-2}). Solvent etching with acetone (5 sec at 274 K) proved to be an excellent method for revealing the emergent ends of growth and mechanically induced dislocations in PETN. Etching of microhardness indentations confirmed that observable slip traces comprised dislocations. These migrated up to 160 μm (20 g load) from the indentation point on both {1 1 0} and {1 0 1} faces. The alignments defined a {1 1 0} primary slip plane. Parallel experiments with RDX yielded evidence of highly localized slip around the indentation mark (90 μm, 50 g load). Two alignments of etch pits were noticeable. The better defined of these lay at the intersection of the (0 1 0) plane with the habit faces. The second could not be defined absolutely but most probably corresponds to the intersection of either the (0 1 1) or (0 1 2) plane with the surfaces. Consideration of the Burgers vectors of dislocations which are likely to glide in these planes lead us to speculate that the primary slip systems are, PETN {1 1 0} [0 0 1], and RDX (0 1 0) [0 0 1]. Such an assignment would be consistent with the relative hardness of the two materials.

1. Introduction

Experimental studies of the sensitivity of energetic materials to initiation by mechanical shock [1–4] has given rise to the speculation that the energy localized during the accompanying plastic deformation may contribute significantly to the initiation process. A mechanism has been proposed whereby dislocations, driven along their slip-planes by the initiating shock wave "pile-up", either against each other or some obstacle [5]. The consequent transfer of strain and kinetic energy to heat within a microscopic region is proposed to form the "hot spot" which nucleates the reaction. Theoretical calculations have been made to confirm that such a model is rational [6]. Unfortunately, little is known of the properties and characteristics of mechanically induced dislocations in this type of material and on which detailed assessments can be based. In an effort to fill this gap, we have commenced a detailed analysis of the defect properties of organic energetic materials. In the present case we detail methods for the etching

*Present address: Department of Engineering Materials, University of Southampton, UK.

0022–2461/84 $03.00 + .12

of the emergent ends of dislocations in pentaerythritol tetranitrate (PETN). Using these coupled with microhardness indentation studies we define for the first time the primary slip planes in this material.

Using previously defined etching techniques a similar comparison is made for the related solid cyclotrimethylene trinitramine (RDX).

2. Experimental details

2.1. Crystal preparation

Crystals of PETN and RDX were grown by slow cooling of the saturated solutions of the multiply recrystallized solid from purified acetone (PETN and RDX) and ethyl acetate (PETN) [7]. The crystals of both solids were prismatic and exhibited well-developed faceting. The principal forms were:

PETN {1 1 0} and {1 0 1}

RDX {2 1 0}, {1 1 1}, {0 0 1}, {0 1 0}, {1 0 0} and {1 0 2}

Complete details of the purification, purity and preparation of the crystals and the variation of morphology and internal perfection with preparation conditions will be given elsewhere [8].

The crystal structures of the two materials are as follows:

PETN tetragonal, space group $P\bar{4}2_1c$

$a = b = 0.938\,\text{nm}, c = 0.670\,\text{nm}, z = 2$ [9]

RDX orthorhombic, space group Pbca

$a = 1.318\,\text{nm}, \quad b = 1.157\,\text{nm},$

$c = 1.071, \quad z = 8$ [10].

2.2. Etching studies

2.2.1. RDX

The etchant devised by Connick and May [11], acetone at 298 K, was used for this material. Etching of as-grown surfaces produced results similar to those noted by these workers. For the etching of indentation marks it was found necessary to reduce the etching time to 1s in order to resolve individual pits.

2.2.2. PETN

As far as we are aware, only a brief note of the uncontrolled solvent etching of this material has been previously published [12]. A number of solvents and mixtures of solvents were assessed. The results are summarized in Table I. Acetone proved to be the most satisfactory etchant. Etching was rapid however and to produce well-defined pits it was found necessary to etch for periods of < 5 sec at 274 K followed by a rapid quench in water at this temperature. The results of this procedure for both {1 0 0} and {1 0 1} habit faces are shown in Figs. 1a, b and c.

Since PETN does not cleave, no comparison of etch patterns on cleavage pairs could be made. The correspondence of etch pits with dislocations is well-defined, however, by their persistence on repeated etching and their association with slip patterns following microhardness indentation (Fig. 3).

2.3. Microhardness measurements

Microhardness studies were carried out using a Leitz Miniload microhardness tester fitted with a Vickers pyramidal indenter. Measurements were

TABLE I Summary of solvent etching experiments for PETN

Solvent	Etching time (sec)	Results
Cyclohexanone	1–20	Hexagonal pits elongated along [0 0 1]. Mostly flat-bottomed. Definition poor.
Toluene	5	Surface roughening – no pits.
Ethyl acetate	1	Semi-regular hexagonal pits mostly overetched but some small pits.
Other actetate and Propionate esters	1	No improvement on ethyl acetate
Methyl ethyl ketone	1	As ethyl acetate.
Acetone	1	Semi-regular hexagonal pits – sharp and well-defined.
Water	up to 2 h	No effect
Acetone/water (various proportions)	1	Reduced pit size compared with acetone but poor definition of pits.
Acetic acid	1	No pits – surface roughening only.

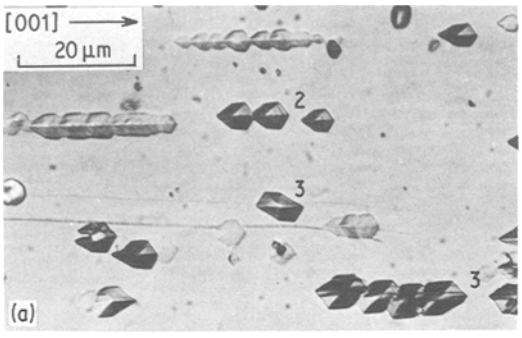

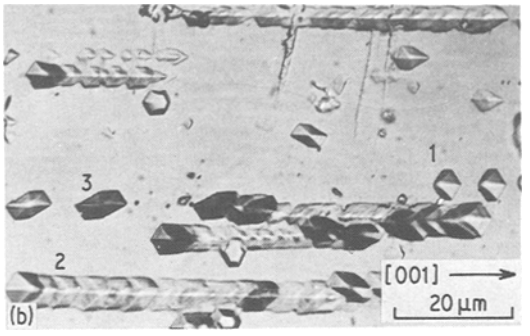

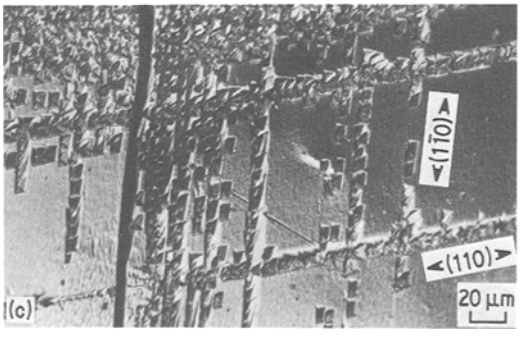

Figure 1 Dislocation etch patterns on (a) and (b) the {110}, and (c) the {101} habit faces of PETN crystals. The numbers denote the three types of dislocation etch-pits discussed in the text.

made as a function of load, temperature and crystal orientation.

3. Results

3.1. Etching studies

3.1.1. PETN

3.1.1.1. {110} faces. Figs. 1a and b show {110} habit faces etched as described above. All pits were hexagonal in surface section and showed three geometries:

type 1, semi-regular hexagonal pits symmetrical about [110];

type 2, hexagonal pits with {110} as the plane of symmetry but elongated in the [001] direction;

type 3, irregularly shaped hexagonal pits with an axis of symmetry normal to the surface.

Flat-bottomed pits were also noted. Types 1 and 2 pits formed [001] alignments predominantly together with some isolated pits. Type 3 pits were predominantly isolated.

All pits initially retained their shape on continued etching. Types 1 and 2 eventually became flat bottomed, type 3 always maintained a point bottom.

Optical and interference microscopy allowed the definition of the geometry of the type 1 and 2 pits as shown in Fig. 2. Type 1 pits are shallow with planar surfaces lying along high index planes. The point is displaced a considerable distance from the geometrical centre, indicating that the dislocation line is inclined at a low angle to the surface. Type 2 pits are similarly shallow but have convex sides. The gradient of these increases towards the point. Although the apex is close to the geometrical centre, the shallowness of the pit implies that the dislocation must again lie at a relatively low angle to the surface. For both pits the combination of shape and alignment confirms that the dislocations must lie in the {110} planes. Type 3 pits differ from 1 and 2 in that the point coincides with the geometrical centre. Thus the dislocation responsible emerges normal to the surface.

A survey of a large selection of etched crystals showed the incidence of pits to be type 1 > type 2 ⩾ type 3. The last form only a few per cent of the total.

3.1.1.2. {101} faces. Etch-pits on these faces were all similarly trapezoidal in surface shape and formed alignments parallel to the intersection of the {110} planes with the face (Fig. 1c). In all cases the points were offset from the geometrical centre (Fig. 2c). The offset angle varied from pit to pit and it was not possible to obtain sufficient definition for interference microscopy. General observation indicated that the dislocation lines must lie in the {110} planes.

3.1.1.3. Possible dislocation types. Three types of growth dislocations in the {110} growth sector have been identified by X-ray topography [13]; **b**[001] edge, **b**⟨100⟩ mixed and **b**⟨111⟩ mixed.

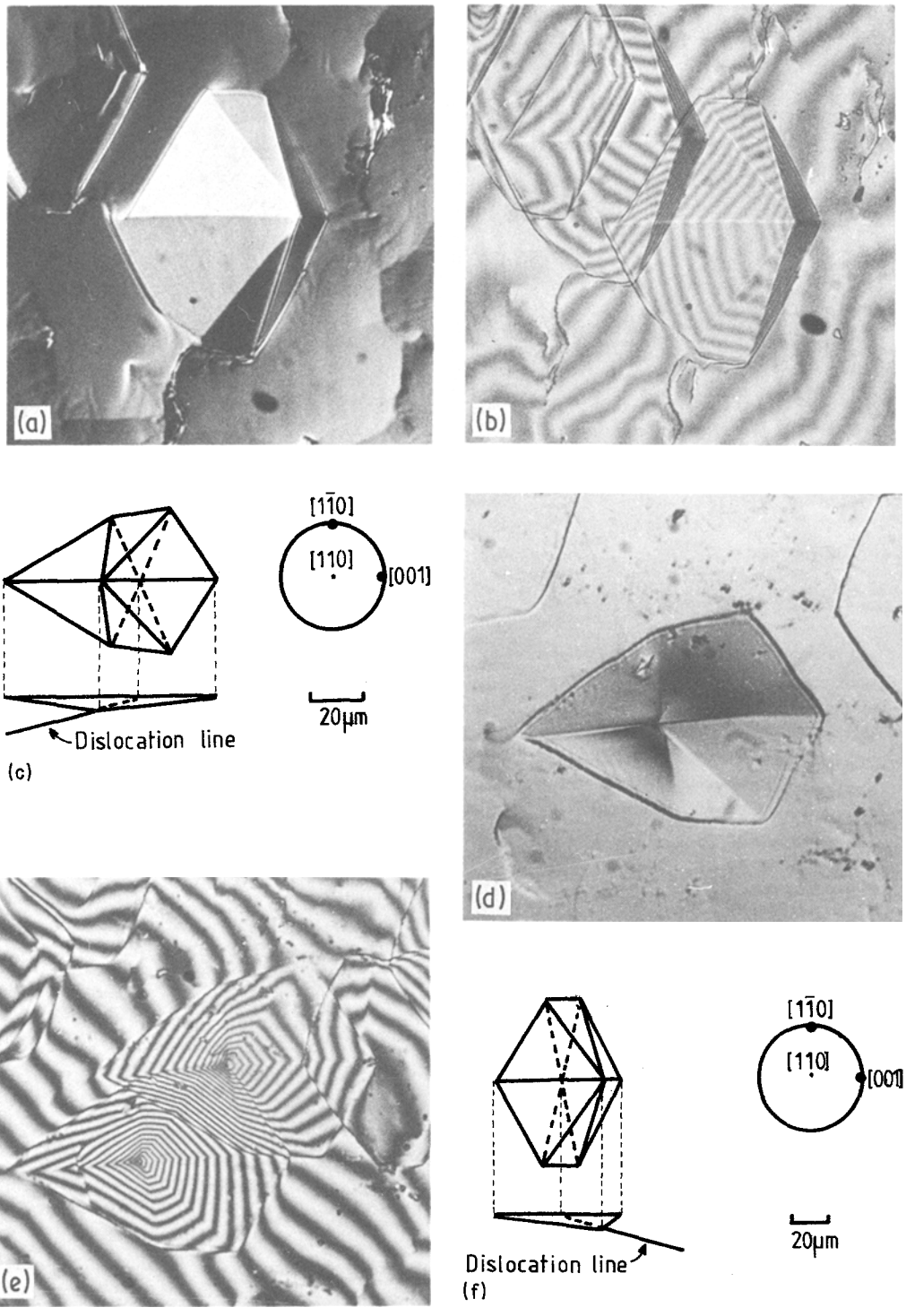

Figure 2 Detailed structure of the etch-pits produced by acetone etching on PETN surfaces. {1 1 0} surface, type 1 pit, (a) optical micrograph, (b) interference micrograph, (c) geometry. {1 1 0} surface, type 2 pit, (d), (e) and (f) as above. (g) Geometry of the pits observed on {1 0 1} surfaces.

Of these, only those with **b**[001] lie normal to the surface and could yield a pit of type 3 geometry. The persistence of this type of pit on continued etching, the small numbers and the fact that it does not usually form part of any alignment is consistent with this interpretation. The other growth dislocations are more highly inclined; **b**⟨100⟩ in the (001) plane at 68° to (110) and **b**⟨111⟩ in the {110} plane at 70° to the face. Pits associable with the former geometry have not been noted. The latter could yield a pit of type 1 or 2 geometry and some of the isolated pits could represent these dislocations. For the most part, however, it is probable that the majority of the types 1 and 2 pits result from dislocations mechanically induced by surface damage during growth and preparation, and which lie in {110} slip planes. Their total numbers far exceed the bulk dislocation content as evidence by X-ray topography ($< 10 cm^{-3}$). Their alignment and the fact that on continued etching, they develop a flat bottom, also is consistent with this interpretation. If so, the low angle to the surface implies only a shallow penetration of the dislocation loops.

Whether or not the types 1 and 2 pits reflect different dislocation types, differences in etching rates or simply different depths of the dislocation loops, is difficult to assess. Their distinctive orientation coupled with their close proximity on the surface does suggest that they result from different mechanical dislocation types.

Confirmation of the mechanical genesis of the majority of etch pits can be derived from the etching studies of the {101} faces. From the topographic studies [13] we know these growth sectors to be highly perfect and the lack of etch pits associable with growth dislocations is not surprising. All etch pits form arrays consistent with shallow, mechanically induced, dislocation loops lying close to the surface in the {110} planes.

In summary, etch patterns on PETN crystal surfaces and their geometries are consistent with the emergence points of known growth dislocation types and with mechanically induced dislocations which glide on {110} slip planes. Further evidence for the latter can be adduced from microhardness measurements.

3.2. Deformation studies

3.2.1. Microhardness measurements

Previous studies of the microhardness of these materials were directed towards the definition of surface energy and crack formation [14]. In these studies evidence for slip in PETN was noted. We have extended this type of measurement in an effort to define the dislocations involved in the process.

3.2.1.1. PETN. The hardness of as-grown {110} and {101} type crystal surfaces was determined as a function of load ({110} and {101}) and temperature, {110}. Indentations made as a function of orientation in the surface revealed slip traces characteristic of localized plastic deformation around the indentation mark together with some cracking (Figs. 3a and c). Both slip and crack directions were constant, independent of indenter orientation. The cracks duplicated, in size and direction, the observations of Hagan and Chaudhri [14] and were not studied further.

Even with careful surface orientation the indentations were not square and straight-sided. This is indirect evidence of anisotropy. The slip patterns produce a curved trough on the surface which distorts the indentation and leads to errors in the measurement. Further errors may also arise as a consequence of the propagation of the surface cracks which will use energy which might otherwise have been utilized in plastic flow. To minimize these errors and to produce comparative data, hardness measurements on {110} surfaces were made with one indenter diagonal parallel to [001] and using the length of the ⟨110⟩ diagonal in the calculations. For similar reasons all measurements on the {101} faces were taken with one diagonal parallel to the trace of [110] on this face.

There was no variation in hardness with load or surface orientation within experimental error. The range, diamond pyramidal hardness, DPH = 15 to $17 kg mm^{-2}$ was in satisfactory agreement with a value quoted by Hagan and Chaudhri.

The lack of variation with load is not surprising. If two indentations have the same shape, then whatever their size, the associated strain field will be identical. Thus hardness will be independent of load. In contrast, variation of hardness with surface orientation is usually expected by virtue of the orientation of the indenter with respect to the slip systems presented on each face. We can only assume that the difference in angle between the direction of indentation and slip plane is compensated for by that between the indentation direction and slip direction or by the availability of two slip systems on the {101} faces.

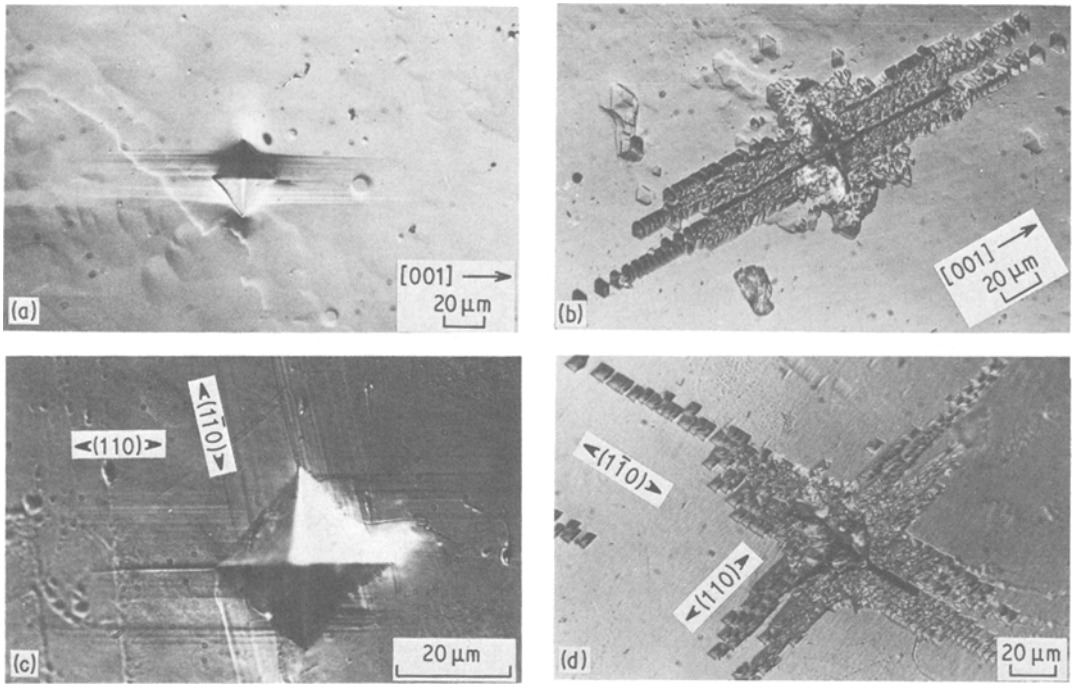

Figure 3 Microhardness impressions (20 g load) on the habit faces of PETN crystals. (a) {1 1 0} surface, (b) {1 0 1} surface. (c) and (d) show (a) and (b) after acetone etching.

The variation in hardness with temperature was small but significant; DPH = 17 to 13 kg mm^{-2} over the range 298 to 323 K. The decrease was gradual and is probably consistent with changes in intermolecular lattice forces with temperature. From this and surface observations, we conclude that only the slip systems operative at ambient temperature remain so up to 323 K. At this temperature surface deterioration due to evaporation and decomposition commences.

3.2.1.2. RDX. Hardness measurements were made as a function of load and temperature on the {2 1 0} faces of RDX. As noted by Hagan and Chaudhri [14] extensive cracking parallel and perpendicular to [0 0 1] accompanied all indentations. No slip lines were observable over the range of loads used. The hardness remained constant with load (DPH = 38 to 39 kg mm^{-2}) but exhibited a smooth decrease with temperature (39 to 27 kg mm^{-2}) in the range 294 to 373 K. Thus it is unlikely that there will be any sudden changes in deformation mechanisms over this range. The hardness value of 39 kg mm^{-2} (294 K) is much higher than that noted by Hagan and Chaudhri (24 kg mm^{-2}) and corresponds to the upper end of a range noted by Elban and Armstrong [15] (32 to 39 kg mm^{-2}). We attribute this to the improved quality of crystals used in the present study.

3.2.2. Etching of microhardness indentations

The indented faces of both PETN and RDX crystals were etched in order to define more clearly the full extent of the plastically deformed regions around the indentations and to provide more information on the densities and configurations of dislocations in these slip planes.

3.2.2.1. PETN. Figs. 3b and d show etched indentations (20 g load) on the (1 1 0) and (1 0 1) faces, respectively. In the former case, type 1 dislocation etch pits spread out from the indentation in lines corresponding to the intersection of a (1 $\bar{1}$ 0) plane with the surface. Interestingly, the pit bottoms show a similar oblique orientation to the surface on both sides of the indentation mark suggesting that they represent the ends of oblique loops of a parallelogram shape. This alignment and the pit orientation define a (1 1 0) slip plane.

This geometry is confirmed by the distribution of pits around the indentation on the (1 0 1) face

(Fig. 3d). These lie in alignments corresponding to the intersection of the (110) and (1$\bar{1}$0) planes with the face. Again the pits show equivalent asymmetry on both sides of the loop. They also show an interesting distribution on each side of the indentation giving a short and long arm in each quadrant implying a considerable anisotropy of the slip process.

3.2.2.2. RDX. Etched indentations (50 g load) on the {210}, {111} and (001) habit faces are depicted in Figs. 4a, b and c. Despite the fact that no slip lines were apparent during the microhardness studies, all reveal dislocation alignments spreading for small distances around the marks.

On the {210} face the dominant alignment is in the [001] direction. It is interesting to note that the rows of pits propagate from the crack C rather than from the indentation itself. Also, they are on one side of the indentation only. This reflects the crystallographic symmetry of the (210) face. A second possible alignment at 30 to 60° to [001] can also be detected at A.

The result of etching an indentation on the (001) face (Fig. 4b) is to yield alignments parallel to [100]. Only one plane, namely (010), could give rise to the principal alignments on the (210) and (001) faces. This defines the slip plane. This assignment is confirmed by the etched indentation on the (111) face where again alignments are produced which correspond to the trace of the (010) plane on this surface.

Although there is some confusion in the latter case due to the etching of cracks which inevitably accompanied indentation on this face, there is a definite indication of a secondary alignment at *X*. Accepting that this is present and returning to Fig. 4a we note that the most probable orientation of alignment A is parallel to the intersection of either the (021) or (011) plane with the face. Both of these planes will intersect the (001) faces in a line parallel to [100] and hence yield no additional alignment. Their intersection with the (111) face are noted on Fig. 4c. Of the two possibilities, this evidence suggests that the most likely secondary slip plane is (011) rather than (021).

The proposal of an (010) primary slip plane is in agreement with the observations of Connick and May [11] following their original etching examination of surface damage on RDX. It conflicts with the results of Elban and Armstrong [15], who propose a {021} primary slip plane following indentation and etching studies of only the {210} faces. It may be that the secondary slip system noted above will be of this orientation. Further assessments of the anisotropy of hardness on these faces are in course in order to resolve this matter.

4. Conclusions

The present examination shows, in confirmation of previous work [14] that PETN is a softer solid than RDX. It proves in addition that this distinction can be associated with the relative ease of dislocation slip in the two materials. In the former, microhardness impressions lead to the emission of

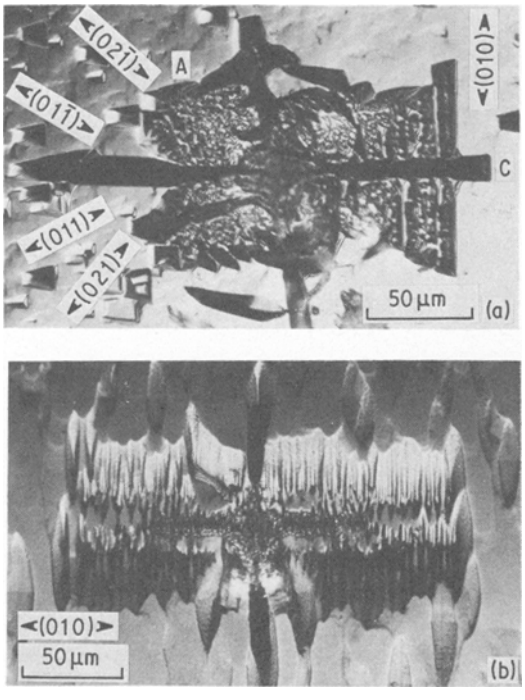

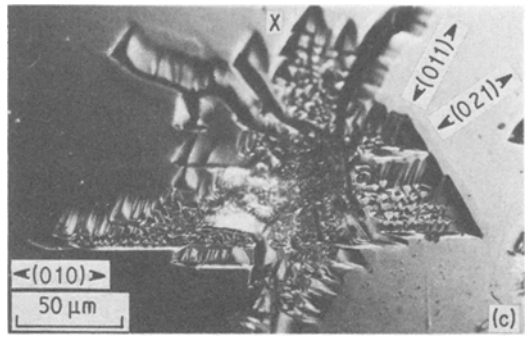

Figure 4 Etched microhardness impressions (50 g load) on the (a) (210), (b) (001), and (c) (111) habit faces of RDX.

well-defined slip-traces along (1 1 0) and (1 $\bar{1}$ 0) slip planes to a distance of 160 μm (20 g load). In the latter, deformation is localized within a much smaller region and along the (0 1 0) planes (90 μm, 50 g load).

If this proposal is correct, then the distinction in plasticity should be reflected in the properties of the dislocations involved in the process. This study defines accurately the slip planes, the direction and magnitude of the Burgers vectors of the component dislocations can only be assessed by speculation.

For PETN, the slip plane is defined as {1 1 0}. The most likely Burgers vectors of pure dislocations which will glide on this plane are [0 0 1], ⟨1 1 0⟩ and ⟨1 1 1⟩ (0.67, 1.32 and 1.486 nm, respectively). These will have line energies ($E_l = kb^2$), where k is the energy factor) of 19, 77 and 103 eV nm^{-1}. The significantly lower energy of the first suggests that the most likely mobile dislocation will be of the type {1 1 0}[0 0 1]. This energy places PETN in the class of a moderately plastic solid but in which the overall plasticity is limited by the number of potential slip systems.

Of the two slip systems noted for RDX, only the (0 1 0) is well defined. This limits the possible dislocations to those with **b**[0 0 1], [1 0 0] and [1 0 1] (1.07, 1.359 and 1.690 nm, respectively). The (0 1 0)[0 0 1] system is most likely configuration. Unfortunately, no elastic constants are available for this material. The bulk modulus cannot be greatly dissimilar, however, to that for PETN. Thus the line energy of dislocations of even the smallest Burgers vector will be considerably greater than that for PETN. Coupled with this, the distortion involved even with a simple [0 0 1] vector in a lattice with eight molecules per unit cell will be considerable and motion of this dislocation will be a complicated and energetic process. The participation of the second slip system and/or motion by partials might facilitate slip. Even then, the reduced energy will still be likely to be much higher than for PETN. The accurate evaluation of such possibilities must await the better and complete definition of the slip systems.

A final question which must be posed relates to the potential involvement of dislocations in the energetic process in these materials. If there is an association, it would be expected to arise from the concentration of mobile dislocations within a microscopic region; their interaction and consequent transfer of energy giving the potential initiating "hot spot". Two factors are noteworthy in this context. Firstly, aside from the single rows of pits far from the indentation, the dislocation density around the indentations in PETN is much greater than for RDX. Additionally, althouth they are mostly inclined to the surface, the dislocations produced by indentations in RDX are not as shallowly inclined as those for PETN. Hence the deformed region in the latter case is confined to a very shallow volume close to the surface. Both factors define that the greater deformation of PETN is confined to a smaller volume than RDX. This concentration could well account for the known greater sensitivity of PETN to impact detonation.

In summary we note that mechanical deformation in PETN proceeds by dislocation motion in the (1 1 0) and (1 $\bar{1}$ 0) slip planes possibly by the motion of {1 1 0}[0 0 1] type dislocations. In RDX primary slip is limited to the (0 1 0) planes and probably involves high energy (0 1 0)[0 0 1] type dislocations. A secondary ill-defined slip system probably occurs on the (0 1 1) or (0 2 1) planes. Simple energetic considerations show that the relative hardness of the two materials can be accounted for by the relative energies of the different dislocation slip systems.

Acknowledgement

We express our grateful thanks to the European Office of the US Army (USARDSG-UK) for their financial support of this work.

Note added in proof: Since completing this work it has been pointed out to us that PETN crystals of small dimensions can show a well-defined cleavage in the {1 1 0} planes [16]. Additionally, Azumu *et al.* [17] have assessed the temperature dependence of microhardness of both PETN and RDX. Our results are in excellent agreement with their findings.

References

1. F. D. BROWN and K. SINGH, *Proc. Roy. Soc. (Lond.)* **A227** (1954) 22.
2. W. E. GARNER, *ibid.* **A246** (1938) 203.
3. S. N. HEAVENS and J. E. FIELD, *ibid.* **A338** (1974) 77.
4. R. E. WINTER and J. E. FIELD, *ibid.* **A343** (1975) 339.
5. C. S. COFFEY and R. W. ARMSTRONG, "Shock Waves and High Strain Rate Phenomena in Metals: Concepts and Applications", edited by M. A. Meyers and L. E. Muir (Plenum Press, New York, 1981).

6. C. S. COFFEY, *Phys. Rev.* **B24** (1981).
7. R. M. HOOPER, B. J. McARDLE, R. S. NARANG and J. N. SHERWOOD, "Crystal Growth, 2nd Edn., edited by B. Pamplin (Pergamon, London, 1980) p. 395.
8. P. J. HALFPENNY, K. J. ROBERTS and J. N. SHERWOOD, *J. Cryst. Growth* (1984) submitted.
9. A. D. BOOTH and F. J. LLEWELLYN, *J. Chem. Soc.* (1947) 837.
10. C. S. CHOI and E. PRINCE, *Acta Crystallogr.* **B28** (1972) 2857.
11. W. CONNICK and F. G. J. MAY, *J. Crystal Growth* 5 (1969) 165.
12. J. J. DICK, *J. Appl. Phys.* **53** (1982) 6161.
13. P. J. HALFPENNY, K. J. ROBERTS and J. N. SHERWOOD, *J. Appl. Crystallogr.* (1984) submitted.
14. J. T. HAGAN and M. M. CHAUDHRI, *J. Mater. Sci.* **12** (1977) 1055.
15. W. ELBAN and R. W. ARMSTRONG, Seventh International Symposium on Detonation, Annapolis, Maryland, 1981 (US Office of Naval Research, Washington, DC, 1981).
16. H. M. HAUSER, J. E. FIELD and V. K. MOHAN, *Chem. Phys. Lett.* 99 (1983) 66.
17. J. K. A. AZUMU, B. J. BRISCOE and M. M. CHAUDHRI, *J. Phys. D. Appl. Phys.* 9 (1976) 133.

Received 22 August
and accepted 13 September 1983